Characterization of Association Colloids of Amphiphilic Poly(*p*-phenylene)sulfonates in Aqueous Solution

M. Bockstaller,[†,‡] W. Köhler,[†] G. Wegner,[*,‡] and G. Fytas[§]

Physikalisches Institut, Universität Bayreuth, D-95440 Bayreuth, Germany; Max-Planck-Institut für Polymerforschung, Postfach 3148, D-55021 Mainz, Germany; and FORTH Institute for Electronic Structure and Laser, P.O. Box 1527, 71110 Heraklion, Crete, Greece

Received January 8, 2001; Revised Manuscript Received June 15, 2001

ABSTRACT: Highly charged dodecyl-substituted poly(*p*-phenylene)sulfonates (PPPs) with molar masses of 12 and 27 kg/mol have been characterized in dilute salt-free aqueous solution. Besides direct visualization by means of transmission electron microscopy, static and dynamic light scattering as well as small-angle X-ray scattering have been employed for the characterization. The PPPs form cylindrical association colloids with similar radii and radial and axial aggregation numbers for both molar masses. These micelles are stable with respect to their radial strand aggregation number over the entire accessible concentration range, and even at the lowest concentration of $c = 0.001$ g/L, no single chains could be observed.

Introduction

Water-soluble polyelectrolytes are of fundamental importance in biology and biochemistry. The ability to self-assemble reproducibly into highly ordered supramolecular structures is essential to the function of biogenic polymers. Hence, understanding and controlling the parameters that determine the structure formation process in aqueous polyelectrolyte solutions is of major scientific interest.[1,2] However, polyelectrolyte systems remain among the least understood systems in macromolecular science. This is due to the complicated coupling of short-range (excluded volume) and long-range (Coulombic) interactions, which are simultaneously present and which result in a complex dependence of physical properties on the local structure of the polymer chains.[3,4] To compare theoretical and experimental results, the inherent structural parameters of the charged macromolecules have to be known, and great effort has been devoted to the synthesis of stiff chain polymers that model the complex properties of biogenic polymers.[5,6] Poly(*p*-phenylene)sulfonates (PPPs) exhibit a chemical bond pattern which inflicts intrinsic stiffness, i.e., chain persistence, to the macromolecule. Substitution of this backbone by hydrophobic and ionizable groups induces self-assembly, in which the chain persistence plays an intrinsic role in addition to Coulombic and hydrophobic interactions.[7] The polyelectrolytes discussed herein have previously been characterized in a precursor state.[8] Polymers with molar masses between 16 and 99 kg/mol had been synthesized, and a persistence length of 13 nm[8] to 15 nm[9] for the single chain has been determined with different techniques. In contrast to the precursors in organic solvents, isolated single chains could not be observed for the corresponding polyelectrolyte in aqueous solution, even at the lowest experimentally accessible concentrations. Hence, the characterization at the precursor state becomes a necessity.

Rulkens et al. have studied semidilute to concentrated aqueous solutions of the PPPs by SAXS and interpreted their results in terms of cylindrical aggregates formed by the amphiphilic PPPs.[10] Later, Liu et al. were able to observe both single chains and spherical micellar aggregates coexisting in methanol and mixtures of water/methanol.[11]

In this contribution, we will present a detailed quantitative characterization of the cylindrical micelles in dilute aqueous solution for two PPPs with different molar masses.

The data are projected onto a model which is sketched in Figure 1. It shows the chemical structure of the dodecyl-substituted PPP sulfonate and the rodlike micelles formed thereof. The aliphatic chains fill the interior of the cylinder and the hydrophilic sulfonate groups are located at the outer surface.

Experimental Section

Materials. The synthesis of hairy rod poly(*p*-phenylene)s with sulfonated side chain groups, with detailed structure as depicted in Figure 1, has been reported elsewhere.[5,12] In the present work, PPPs as shown in Figure 1 of molar mass 12 and 27 kg/mol (abbreviated PPP12 and PPP27) with similar polydispersity $M_W/M_N \approx 2.0$ have been studied. To remove impurities, PPPs were dissolved in water and dialyzed for 3 days against deionized Milli-Q water with a resistivity of 18.2 MΩ·cm. After freeze-drying, solutions were prepared by dissolving the appropriate amount of PPPs in deionized water under continuous stirring for several hours. Concentrations below $c = 0.1$ g/L were prepared by dilution of concentrated solutions. Dust-free solutions were subsequently obtained by filtration through a 0.45 μm cellulose acetate filter (Millipore).

Photon Correlation Spectroscopy (PCS). The autocorrelation function $g_2(q,t)$

$$g_2(q,t) = \frac{\langle I(q,0)\, I(q,t)\rangle}{\langle |I(q,0)|^2\rangle} \tag{1}$$

of the light scattering intensity $I(q)$ at a scattering vector $q = 4\pi n\lambda^{-1} \sin(\theta/2)$ (n is the refractive index of the medium, λ is the vacuum wavelength of the incident light, and θ is the scattering angle with $12° \le \theta \le 150°$) was measured with an automated ALV goniometer and an ALV-5000 full digital correlator (320 channels) over the time range $10^{-7} \le t \le 10^3$ s.

[†] Universität Bayreuth.
[‡] Max-Planck-Institut für Polymerforschung.
[§] FORTH Institute for Electronic Structure and Laser.
* Corresponding author.

10.1021/ma010026q CCC: $20.00 © 2001 American Chemical Society
Published on Web 07/31/2001

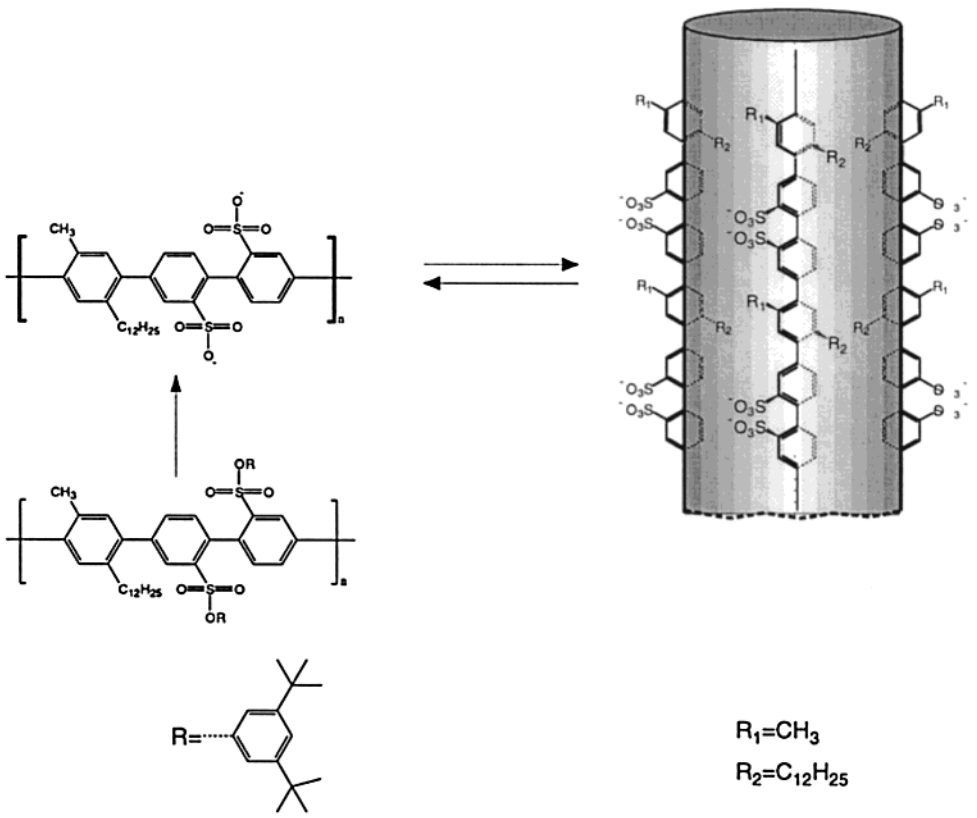

Figure 1. Chemical structure of the polyelectrolyte and schematic representation of the micelles with the hydrophobic side chains oriented toward the interior of the cylinder.

The light source was a Neodym-YAG dye-pumped, air-cooled laser (Adlas DPY 325) with a single mode intensity of 100 mW at $\lambda = 532$ nm. For measurements of the polarized (VV) and depolarized (VH) light scattering intensity, the scattered light was polarized vertically (V) and horizontally (H) with respect to the scattering plane by means of a Glan-Thompson analyzer with an extinction ratio better than 10^{-7}. The polarization of the incident laser beam was vertical (V) in both cases. The normalized light scattering intensity autocorrelation function $g_2(q,t)$ is computed from the Siegert relation[13]

$$g_2(q,t) = 1 + f^*|\alpha g_1(q,t)|^2 \tag{2}$$

where f^* is an experimental instrument factor which relates the scattering area to the coherence area and is determined by means of a standard. α is the fraction of the total scattered intensity arising from fluctuations with correlation times longer than 10^{-7} s.

$$g_1(q,t) = \frac{\langle E^*(q,0)\, E(q,t)\rangle}{\langle |E(q,0)|^2\rangle} \tag{3}$$

is the normalized correlation function of the scattered electric field $E(q,t)$.

For analysis of the experimental correlation function $C(q,t) = \alpha g_1(q,t)$, we have employed inverse Laplace transform using the constraint regularized CONTIN method.[14] This method assumes that $C(q,t)$ can be represented by a superposition of exponentials,

$$C(q,t) = \int_{-\infty}^{\infty} H_\tau(\ln \tau) \exp[-t/\tau]\, \mathrm{d}(\ln \tau) \tag{4}$$

which determines a continuous spectrum of relaxation times $H_\tau(\ln \tau)$. The characteristic relaxation times correspond to the maxima of $H_\tau(\ln \tau)$.

All measurements were carried out at 20 °C. Static light scattering experiments were performed with the same goniometer. Doubly distilled and filtered toluene was used as standard to evaluate absolute scattering intensities. Values of absolute scattered intensities are given in terms of the reduced Rayleigh ratio $R(q)/(Kc)$, with the Rayleigh ratio $R(q)$ given by $R(q) = (\langle I\rangle - \langle I_{\mathrm{solvent}}\rangle)\langle I_{\mathrm{toluene}}\rangle^{-1} I^{\mathrm{abs}}_{\mathrm{toluene}}(90^\circ)\text{-}(n_{\mathrm{solvent}}/n_{\mathrm{toluene}})^2 \sin\theta$, where c is the concentration and n is the refractive index. $K = (2\pi n\, \partial n/\partial c)^2 (N_A \lambda^4)^{-1} = 58.4 \times 10^{-6}$ cm^2 g mol^{-1} is an optical constant,[15] N_A is Avogadro's number, and $\partial n/\partial c$ is the refractive index increment.

Small-Angle X-ray Scattering (SAXS). The SAXS measurements were performed using the synchrotron facility at DESY (HASYLAB), Hamburg, Germany, with $\lambda = 0.15$ nm, $\Delta E/E = 10^{-3}$, and a double focusing camera. For photon counting, an array detector was employed. The form factor of the hollow cylinder has been computed with the aid of the software package SOLPRO.[16]

Electron Microscopy. Imaging of specimen was performed using a PHILIPS CM 10 electron microscope with a LaB6 cathode and 100 kV accelerating voltage. Data were stored using photographic film Ilford PanF. For cryofixation of the specimen, 1 μL of aqueous solution was frozen in liquid propane (−85 °C) using a Balser instruments cryostat. After fracture and etching, the surface was contrasted by shadowing (Pt/C, 45°). All measurements have been performed at the TEM facilities of TU Munich with kind support of R. Merkel and I. Sprenger.

Results and Discussion

Transmission Electron Microscopy. A first hint that the rodlike micelles, as observed by Rulkens et al.[17] in concentrated solutions, exist even down to extremely low concentrations was obtained from electron microscopy.

TEM images after cryofixation of aqueous solutions have been taken both from highly (0.005 g/L) and moderately dilute (0.5 g/L) samples. Figure 2 shows a single highly anisotropic object of approximately 250 nm

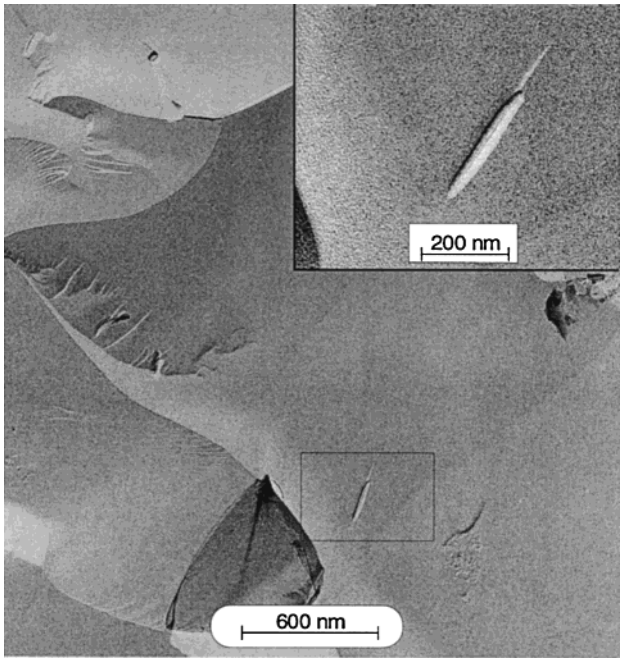

Figure 2. Transmission electron micrograph of PPP27 in aqueous solution at $c = 0.005$ g/L after freeze fracture. The enlarged section shows a single cylindrical micelle.

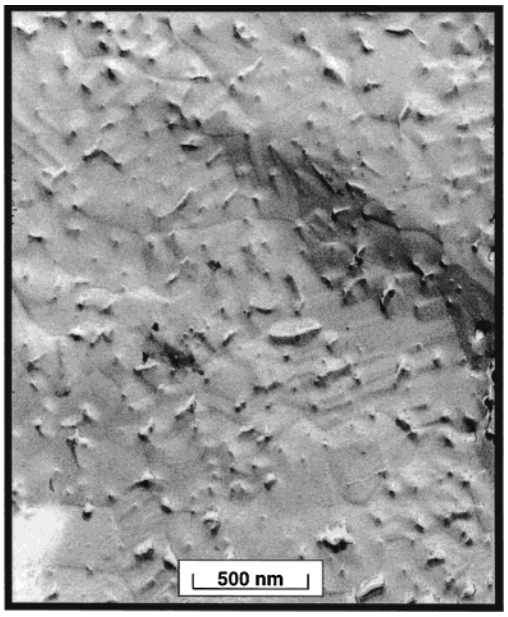

Figure 3. Transmission electron micrograph of PPP27 in aqueous solution at $c = 0.5$ g/L after spray freezing.

length after freeze fracture of a solution of PPP27 at a concentration of 0.005 g/L. Based on the results of the characterization of the precursors,[8] its length clearly exceeds the length of a single chain, which is of the order of 50 nm.

Even at a 100-fold higher concentration of 0.5 g/L, objects of similar size and shape are still prevalent. Figure 3 shows a TEM image obtained from a solution of this concentration after spray freezing. The TEM micrographs confirm our model of long and thin cylindrical micelles as sketched in Figure 1 without revealing, however, any internal structure. Also, a correct estimation of the length distribution is complicated by the small and not necessarily representative number of observed objects and a possible underestimation due to the projection of the orientational distribution onto the observation plane.

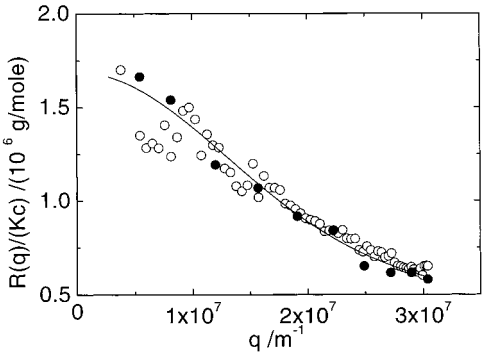

Figure 4. Angular dependence of the reduced Rayleigh ratio $R(q)(Kc)^{-1}$ as obtained from static scattering experiments (open symbols) and from the integration of the respective diffusion mode in dynamic scattering experiments (solid symbols). Sample PPP12, $c = 0.005$ g/L. The solid line is the scattering function of a rigid rod of length $L = 260$ nm according to eq 5.

To resolve these problems and limitations and to gain further insight into the radial structure of the aggregates, we resort to scattering techniques. Nevertheless, the TEM micrographs allow us to select the correct geometrical shape of the objects for the analysis of the scattering data. Without this visual information, the unambiguous selection of the proper form factor would be very difficult due to polydispersity and experimental noise.

Static Light Scattering. Because of the low q range employed in our light scattering experiments, information about the average overall length and molar mass of the association colloids can be obtained without prior knowledge about their radial structure, as long as the diameter is negligible compared to q^{-1}.

Figure 4 shows the angular dependence of the excess scattered intensity of sample PPP12, plotted as $R(q)(Kc)^{-1}$, as a function of the scattering vector. The open symbols correspond to a direct measurement of the total scattered intensity, whereas the solid ones have been extracted from photon correlation spectroscopy data (see below). The solid line is the form factor of a monodisperse thin rod of length $L = 260$ nm and negligible diameter:[18]

$$P_r(qL) = \frac{2}{qL}\int_0^{qL}\frac{\sin z}{z}\,\mathrm{d}z - \left(\frac{\sin qL/2}{qL/2}\right)^2 \qquad (5)$$

The concentration dependence of the extrapolated values $Kc/R(q\rightarrow 0)$ is plotted as a function of concentration in Figure 5. Extrapolation to $c = 0$ yields a weight-average molar mass of the micelles of $M_W = 2.1 \times 10^6$ g/mol for PPP12. From the slope, the second virial coefficient $A_2 = 7.7 \times 10^{-5}$ L mol g^{-2} is obtained.[19] The same procedure for PPP27 yields $M_W = 3.7 \times 10^6$ g/mol and $A_2 = -1.84 \times 10^{-5}$ L mol g^{-2}. The concentration dependence of $Kc/R(q\rightarrow 0)$ is shown together with the values for PPP12 in Figure 5.

Surprisingly, we find a negative A_2 in the case of the higher molar mass sample PPP27, indicative of attractive interactions. For PPP12, A_2 is positive and the interaction repulsive. This different concentration dependence in the dilute regime is already indicative for a significant difference in the complex association patterns that can be observed for both systems at higher concentrations. We will treat these phenomena, which

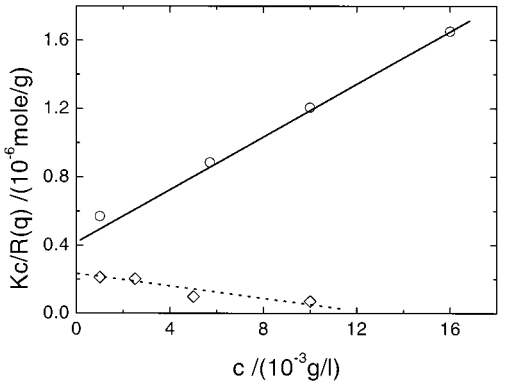

Figure 5. Concentration dependence of $Kc/R(0)$ for PPP12 (○) and PPP27 (◇).

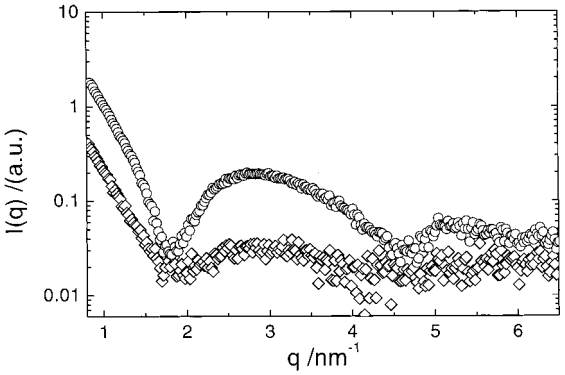

Figure 6. SAXS intensities as a function of q for PPP12 at c = 2.87 g/L (◇) and c = 18.6 g/L (○).

are beyond the scope of the dilute solution properties treated in this paper, in a forthcoming publication. Polydispersity effects have been neglected in eq 5. Below, we will extract the length distribution from photon correlation spectroscopy measurements.

Small-Angle X-ray Scattering. Information about the diameter of the cylindrical micelles can be obtained from scattering at the higher q range, as accessible by SAXS. Because of the low scattering contrast of the dilute solutions, most experiments were performed at the DESY synchrotron facility. Figure 6 shows the q dependence of the scattered intensity for two different concentrations of $c = 2.8$ g/L and $c = 18.6$ g/L for PPP12. Obviously, the change in concentration changes the intensity by a factor of approximately 6.6, which is very close to the ratio of the two concentrations employed. The general features displayed by the curves do, however, not change with concentration. There is a first pronounced minimum at $q = 1.7$ nm^{-1}, a maximum at $q = 2.9$ nm^{-1}, a second minimum at $q = 4.5$ nm^{-1}, and another less pronounced maximum around $q = 5.3$ nm^{-1}. This is a clear indication that the observed phenomena are a signature of the form factor of the single micelles.

Figure 7 shows intensity distribution for the high concentration of Figure 6 together with the form factor of a hollow cylinder of inner diameter $d_i = 3.1$ nm and outer diameter $d_o = 3.4$ nm. The model of a hollow cylinder has been employed to account for the low scattering cross section of the aliphatic chains in the center and the high scattering cross section of the sulfonate groups at the periphery. Also plotted in Figure 7 is the corresponding form factor of a homogeneous cylinder of $d = 3.4$ nm diameter:[20]

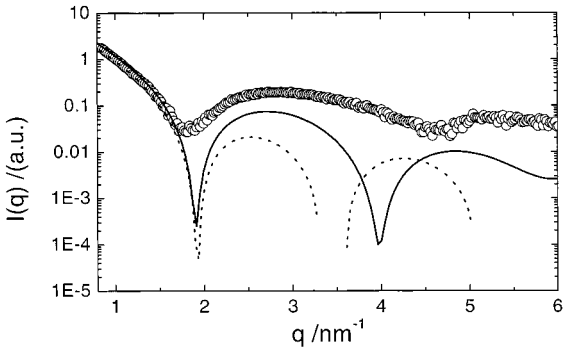

Figure 7. SAXS intensity as a function of q for PPP12 at c = 18.6 g/L (○), adjusted scattering function of a hollow cylinder of length $L = 260$ nm and diameter $d = 3.4$ nm (solid line), and of a homogeneous cylinder of same size (dashed line).

$$P_c(qL) = \int_0^{\pi/2} \frac{\pi}{X}\left(\frac{2J_1(X/2)\ J_1(Y)}{Y}\right)^2 \sin\beta\ \mathrm{d}\beta \qquad (6)$$

J_1 is the Bessel function of the first kind and first order, $X = qL\cos\beta$, and $Y = q(d/2)\sin\beta$. The length $L = 260$ nm does not follow from the SAXS measurements but has been determined by static light scattering.

While the first minima coincide for both models, the position of the second minimum is much better reproduced by the form factor of the hollow cylinder. The vertical shift between the measured data and the computed form factors is probably due to polydispersity, which has not been accounted for, and some background scattering of unknown origin. Independent of molar mass, an identical diameter of 3.4 nm is obtained for both polymers PPP12 and PPP27.

Photon Correlation Spectroscopy. In photon correlation spectroscopy, the intensity autocorrelation function $g_2(q,t)$ (eq 1) is measured, from which the field autocorrelation function $g_1(t)$ can be calculated via the Siegert relation (eq 2). Since we expect the presence of optically anisotropic scatterers, we employed polarized (VV) as well as depolarized (VH) scattering geometries to obtain information about the translational D and rotational D_r diffusion coefficients, respectively.[21] These coefficients of a monodisperse solute in the limit of infinite dilution, where the individual scatterers move independently from each other, are related to $g_1(q,t)$ by

$$g_1^{VV}(q,t) = \exp(-Dq^2t) \qquad (7)$$

$$g_1^{VH}(q,t) = \exp(-[Dq^2 + 6D_r]t) \qquad (8)$$

Polarized Scattering. In the case of polydisperse solutes, the inverse Laplace transform of $g_1(q,t)$ yields the distribution $H_\tau(\ln\tau)$ (eq 4), where $\tau = (Dq^2)^{-1}$ for VV and $\tau = (Dq^2 + 6D_r)^{-1}$ for VH geometry. Once $H_\tau(\ln\tau)$ is known, the length distribution $H_L(L)$ of the cylindrical scatterers can be calculated:

$$H_L(L) = H_\tau(\ln\tau)\left|\frac{\mathrm{d}L}{\mathrm{d}\ln\tau}\right|^{-1} \qquad (9)$$

For VV geometry, L and τ are related via the expression for the translational diffusion coefficient of a solid cylinder in a solvent with viscosity η_0:[22]

$$D = \frac{k_B T}{3\pi\eta_0 L}\left(0.58 + \ln\frac{L}{d}\right) \qquad (10)$$

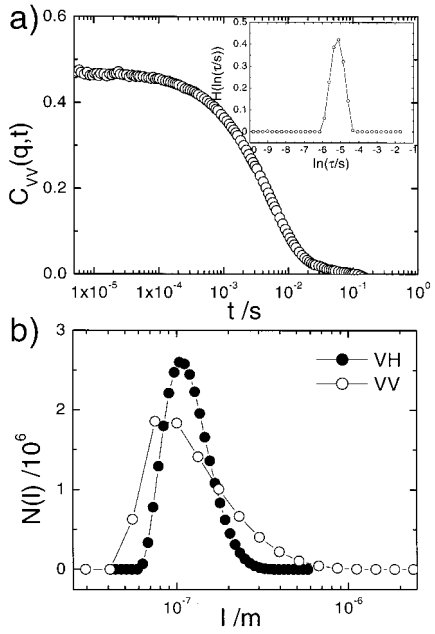

Figure 8. (a) Polarized field autocorrelation function $g_1^{VV}(t)$ for PPP12 at $c = 0.005$ g/L and $q = 8.31 \times 10^6$ m^{-1}. The insert shows the distribution function of the diffusion times $H_\tau(\ln \tau)$. (b) Frequency distribution of micellar length $N_L(L)$ as determined from polarized (○) and depolarized (●) dynamic light scattering.

The contribution of micelles of length L to $g_1^{VV}(q,t)$ is related to the micellar size and concentration by

$$H_L(L) \propto N_L(L)(d^2L)^2P_r(qL) \tag{11}$$

$N_L(L)$ is the number density of micelles of length L. The diameter has been taken constant $d = 3.4$ nm as determined from the SAXS measurements.

Figure 8 shows $C^{VV}(q,t)$ of a $c = 0.005$ g/L solution of PPP12 at $q = 8.31 \times 10^6$ m^{-1} together with the corresponding diffusion time distribution $H_\tau(\ln \tau)$ and the length distribution of the micelles $N_L(L)$. From $N_L(L)$ various averages of the micellar length, assuming constant diameter, are obtained: $L_N = \sum_i N_i L_i (\sum_i N_i)^{-1} = 104$ nm, $L_W = \sum_i N_i L_i^2 (\sum_i N_i L_i)^{-1} = 210$ nm, and $L_Z = \sum_i N_i L_i^3 (\sum_i N_i L_i^2)^{-1} = 269$ nm. There is a good agreement between L_Z from PCS and the length $L = 260$ nm as estimated from the angular dependence of the static scattering intensity (Figure 4).

For the polymer with the higher molar mass, PPP27, a similar analysis yields $L_N = 280$ nm, $L_W = 420$ nm, and $L_Z = 670$ nm.

Once the molar mass M and the length L of the rods are known, the radial aggregation number N_{rad}, which is the average number of polymer chains penetrating the cross section of the cylinder (Figure 1), can be estimated:

$$N_{rad} = \frac{M_W}{L_W}\frac{L_{mono}}{M_{mono}} \tag{12}$$

$L_{mono} = 1.1$ nm and $M_{mono} = 485$ g/mol are the length and molar mass of the monomer unit, respectively. For the two polymers PPP12 and PPP27, $N_{rad} = 17$ and $N_{rad} = 15$ are obtained, which are considered to be identical within the experimental error. Obviously, the radial aggregation number is determined by steric constraints of the polar ionic groups and the packing density of the aliphatic side chains, which must fill the interior of the cylinder. Both do not depend on molar mass and, hence, are identical for PPP12 and PPP27.

Since the polyelectrolytes have been characterized extensively in their uncharged precursor state,[8] the length of the single polymer chains is known to be $\langle L_{poly}\rangle_N = 21$ nm for PPP12 and $\langle L_{poly}\rangle_N = 53$ nm for PPP27. Thus, the axial aggregation number $N_{ax} = L_N/\langle L_{poly}\rangle_N$ along the axis of the cylinder assumes the values 5.5 for PPP12 and 5.0 for PPP27, being very similar for both polymers. The independence of the axial aggregation number from the molar mass is much more difficult to rationalize than the constant N_{rad}. As a consequence of the molar mass independence of N_{rad} and N_{ax}, the total strand aggregation number of the micelles is obtained as approximately 85, independent of the molar mass of the constituting polymer chains. This gives rise to questions and speculations about the influence of the configuration of the chains at the both ends of the micelles and their influence on the stability of the micellar aggregates. The experimental evidence available at present does not allow to give conclusive answers to these questions.

Depolarized Scattering. Similar considerations as for $g_1^{VV}(q,t)$ can be applied to the depolarized field autocorrelation function $g_1^{VH}(q,t)$ (eq 8). At dilute solutions, the depolarization ratio is low (≈0.01), and hence, the anisotropic scattering does not affect the polarized light scattering intensity. In the limit $q \to 0$, orientation fluctuations relax by rotational diffusion and the relaxation time becomes q-independent.[23] Using the rotational diffusion coefficient of a cylindrical object[21]

$$D_r = \frac{k_B T}{\pi\eta_0 L^3}3(\delta - \zeta) \tag{13}$$

where $\delta = \ln(L/d)$ and $\zeta = 1.45 - 7.5(\delta^{-1} - 0.27)^2$,[24] the length distribution can be calculated in a procedure similar to the one employed above for translational diffusion. Because of the lower signal-to-noise ratio of the depolarized scattering, there is a considerable uncertainty in $g_1^{VH}(q,t)$, but the resulting length distribution is in good agreement with the one obtained from the polarized scattering and is included in Figure 8. It gives an additional independent size estimation and confirms the results obtained in the VV geometry. It is worth mentioning that D_r ($\propto L^{-3}$, eq 13) is more sensitive to the length polydispersity than D ($\propto L^{-1}$, eq 10).

Summary and Conclusions

In this paper we have shown that dodecyl-substituted PPPs in dilute aqueous solution self-assemble into highly anisotropic micelles of cylindrical symmetry. From transmission electron microscopy after cryofixation, from static and dynamic istotropic and anisotropic light scattering, and from SAXS measurements, a quantitative characterization of these aggregates has been possible. For the two polymeric samples PPP12 and PPP27 of identical chemical structure and different molar mass of the constituting polymer chains, the molar mass, the diameter, the average length, and the length distribution have been determined.

The fundamental problem of determining the correct form factor of a polydisperse sample without a priori knowledge of the geometry of the scatterers was resolved by direct imaging of the solute in the undisturbed

Table 1. Characteristic Dimensions of the Association Colloids

	PPP12			PPP27		
	SLS	DLS	SAXS	SLS	DLS	SAXS
$\langle L\rangle$/nm	260			500		
$\langle L\rangle_N$/nm		104			280	
$\langle L\rangle_W$/nm		210			420	
$\langle L\rangle_Z$/nm		269			670	
d/nm			3.4			3.4
$\langle M\rangle_W$/(g/mol)	2.1×10^6			3.6×10^6		
N_{rad}	17			15		
N_{ax}	5.5			5		

state using TEM in combination with cryofixation techniques. The scattering experiments, on the other hand, allowed for the determination of well-defined averages of mass, diameter, length and, from the Laplace inversion of the time dependence of the correlation functions, an estimation of the length distribution function.

After the proper averages had been determined, the radial aggregation number could be calculated. Since the length of the individual chains was already known from a thorough characterization of the nonionic precursor polymers, it was also possible to determine the axial aggregation number and the total number of chains per micelle. All results are summarized in Table 1.

The radial aggregation numbers are in good agreement with results obtained by Rulkens et al. for the same polymer of different molar mass and at higher concentrations.[17] Their value of $N_{rad} = 15$ indicates that the micelles are stable with respect to their radial aggregation number over a broad concentration range.

The strong influence of the solvent polarity is apparent when comparing our results with the findings of Liu et al.[11] They studied the solution properties of the same polymer in methanol and interpreted their results as a coexistence of single polymer chains and spherical aggregates. In aqueous medium, however, no single chains could be observed even at the lowest experimentally accessible concentrations of $c = 0.001$ g/L. Even there, the scattering is completely determined by the presence of the cylindrical association colloids. All experiments reported here have been conducted with salt-free solutions. Addition of low molecular salt does not significantly influence the observed aggregation properties.

Somewhat surprising is the apparently molar mass independent constant axial aggregation number. Contrary to the constant radial aggregation number, no simple explanation can be given at this time. To confirm this finding, more experiments with different molar masses of the PPPs are necessary. With increasing concentration, the physical properties of both samples differ strongly from each other. A first hint is already obtained from the different sign of the second virial coefficient A_2 in the static light scattering experiments on dilute solutions reported in this contribution. This indicates that the effective interactions between the highly charged cylindrical micelles in aqueous solutions depend on the micellar length. As a consequence, these micelles show rather complex hierarchical association patterns at higher concentrations, which will be discussed in a forthcoming publication.

Acknowledgment. The authors thank I. Sprenger and R. Merkel from the Department of Physics at the TU Munich for their kind help with the electron microscopy. The work was supported by the Deutsche Forschungsgemeinschaft, Grants Ko1541 and Schu1047, and by the Max-Planck Society.

References and Notes

(1) Rees, D. A. *Adv. Carbohydr. Chem.* **1969**, *24*, 267.
(2) Laufer, N. *Nature* **1958**, *181*, 1338.
(3) Barrat, J. L.; Joanny, J. F. *Adv. Chem. Phys.* **1996**, *94*, 1.
(4) Barrat, J. L.; Boyer, D. *J. Phys. 2* **1993**, *3*, 343.
(5) Rulkens, R.; Wegner, G.; Enkelmann, V.; Schulze, M. *Ber. Bunsen-Ges. Phys. Chem.* **1996**, *100*, 707.
(6) Brodowski, G.; Horvath, A.; Ballauff, M.; Rehan, M. *Macromolecules* **1996**, *29*, 6962.
(7) Ballauff, M. *Angew. Chem.* **1989**, *101*, 261.
(8) Vanhee, S.; Rulkens, R.; Lehmann, U.; Rosenauer, C.; Schulze, M.; Köhler, W.; Wegner, G. *Macromolecules* **1996**, *29*, 5136.
(9) Petekidis, G.; Vlassopoulos, D.; Fytas, G.; Fleischer, G. *Macromolecules* **1998**, *31*, 1406.
(10) Rulkens, R.; Wegner, G.; Thurn-Albrecht, T. *Langmuir* **1999**, *15*, 4022.
(11) Liu, T.; Rulkens, R.; Wegner, G.; Chu, B. *Macromolecules* **1998**.
(12) Bockstaller, M.; Köhler, W.; Wegner, G.; Fytas, G. *Macromolecules* **2000**, *34*, 6359.
(13) Brown, W., Ed.; *Dynamic Light Scattering;* Clarendon Press: Oxford, 1993.
(14) Provencher, S. W. *Computer Phys. Commun.* **1982**, *27*, 229.
(15) Kratochvil, P. *Classical Light Scattering from Polymer Solutions;* Elsevier: Amsterdam, 1987.
(16) Diaz, F. G.; Lopez, C. J. J.; de la Torre, J. G. *J. Biochem. Biophys. Methods* **1993**, *26*, 261.
(17) Rulkens, R.; Wegner, G.; Thurn-Albrecht, T. *Langmuir* **1999**, *15*, 4022.
(18) Higgins, J.; Benoit, H. *Polymers and Neutron Scattering;* Oxford University Press: Oxford, 1996.
(19) Benmouna, M.; Reed, W. F. Theoretical Developments in Static Light Scattering from Polymers. In *Light Scattering—Principles and Development*; Brown, W., Ed.; Clarendon Press: Oxford, 1996.
(20) Schmitz, K. *An Introduction to Dynamic Light Scattering by Macromolecules*; Academic Press: New York, 1990.
(21) Pecora, R.; Berne, B. *Dynamic Light Scattering;* Wiley Interscience: New York, 1976.
(22) Tsvetkov, V. N. *Rigid-Chain Polymers;* Consultants Bureau: New York, 1989.
(23) Fytas, G.; Patkowski, A. Dynamic Light Scattering from Polymers in Solution and Bulk. In *Dynamic Light Scattering*; Brown, W., Ed.; Clarendon Press: Oxford, 1993.
(24) Pecora, R. *Dynamic Light Scattering;* Plenum Press: New York, 1985.

MA010026Q